Physics of Atomic Nuclei, Vol. 67, No. 10, 2004, pp. 1810–1817. From Yadernaya Fizika, Vol. 67, No. 10, 2004, pp. 1838–1844.

Proceedings of the International Conference "Nuclear Structure and Related Topics"

Structures and Decay of Deep-Hole States in Light Nuclei Populated by the $(p, 2p)$ Reactions*

M. Yosoi[1)], H. Akimune[2)], I. Daito[3)], H. Ejiri[4)], H. Fujimura[3)], M. Fujiwara[3)], K. Hara[3)], K. Y. Hara[2)], T. Ishikawa[1),5)], M. Itoh[3)], Y. Itow[6)], T. Kawabata[3),7)], K. Kobayashi[6)], M. Nakamura[1)], T. Noro[8)], E. Obayashi[3)], H. Sakaguchi[1)], Y. Sakemi[3)], M. Shiozawa[6)], H. Takeda[1),9)], T. Taki[1)], A. Tamii[3)], H. Toyokawa[4)], N. Tsukahara[1)], M. Uchida[3)], T. Yamada[10)], Y. Yasuda[1)], H. P. Yoshida[3)], and R. G. T. Zegers[3),11)]**

Received January 21, 2004

Abstract—Decay particles from the s-hole states in ^{11}B and ^{15}N have been measured in coincidence with the quasifree ^{12}C$(p, 2p)$ and ^{16}O$(p, 2p)$ reactions at $E_p = 392$ MeV. Triton decay is found to be dominant for the ^{11}B(s-hole) state and also found to be larger than α decay for the ^{15}N(s-hole) state despite its smaller Q value compared to α decay. Measured decay branching ratios are discussed in comparison with the results of statistical-model, $SU(3)$-model, and shell-model calculations. The energy spectra around the s-hole states in both ^{11}B and ^{15}N exhibit some bumplike structures, which can be qualitatively explained by recent shell-model calculations for both nuclei. © *2004 MAIK "Nauka/Interperiodica"*.

1. INTRODUCTION

Quasifree scattering is one of the most direct ways of investigating both the single-particle properties in a nucleus and the nature of the strong interaction in the nuclear medium. The first kind of quasifree scattering reaction to be studied extensively was of the form $^{A}Z(p, 2p)^{A-1}(Z-1)$, which is then interpreted as a direct knockout of a proton bound in the ^{A}Z nucleus by a fast incident proton, and the $^{A-1}(Z-1)$ remains in a one-hole state. After the first $(p, 2p)$ experiment by Chamberlain and Segrè [1], quasifree proton knockout reactions were systematically measured using proton beams at medium energies [2, 3] and, later, plenty of quasifree $(e, e'p)$ investigations were also performed [4]. However, for deep-hole states, only the macroscopic structures like separation energies ($E_{\rm sep}$) and total widths (Γ) are obtained. Detailed structures and fragmentation mechanisms of deep-hole states have been little known even for light nuclei until now, while interests in decay characters of s-hole states in light nuclei have been newly aroused through the study of the production of hypernuclei [5, 6] and the relation to the nucleon decay search [7, 8].

The $1s$-hole states are observed as broad bumps in the highly excited energy region above 20 MeV. It is estimated that the ratio of the nuclear radius to the mean free path of a $1s$ hole is about or less than 1 in p-shell nuclei and larger than 1 in heavy nuclei [9]. These results indicate that the s-hole states in light nuclei may have large escape widths ($\Gamma^{\uparrow}$) and that the spreading widths ($\Gamma^{\downarrow}$) are dominant in heavy nuclei. Yamada *et al.* [9] recently calculated spectroscopic factors and partial decay widths for two-body cluster decay processes from the doorway s-hole states of ^{11}B and ^{15}N in the framework of the microscopic cluster model with $SU(3)$ wave functions. The description of the s-hole state is based on the fact that the doorway s-hole state produced by the

*This article was submitted by the authors in English.

[1)]Department of Physics, Kyoto University, Kyoto, Japan.
[2)]Department of Physics, Konan University, Kobe, Japan.
[3)]Research Center for Nuclear Physics, Osaka University, Osaka, Japan.
[4)]Japan Synchrotron Radiation Research Institute, Sayo, Hyogo, Japan.
[5)]Present address: Laboratory of Nuclear Science, Tohoku University, Sendai, Japan.
[6)]Institute for Cosmic Ray Research, University of Tokyo, Kashiwa, Japan.
[7)]Present address: Center for Nuclear Study, University of Tokyo, Hongo, Tokyo, Japan.
[8)]Department of Physics, Kyushu University, Fukuoka, Japan.
[9)]Present address: RI Beam Science Laboratory, RIKEN, Wako, Japan.
[10)]Laboratory of Physics, Kanto Gakuin University, Yokohama, Japan.
[11)]Present address: NSCL/MSU, East Lansing, USA.
[**]e-mail: yosoi@ne.scphys.kyoto-u.ac.jp

quasifree knockout reactions should have the same spatial symmetry as the ground state of the target nucleus, whose wave function is well described by the $SU(3)$-cluster model in light nuclei. The authors showed in their $SU(3)$-model calculation that a selection rule owing to the spatial symmetry is valid for fragmentation of s-hole states in light nuclei: n, p, d, t, and ^{3}He fragments are allowed, while fragments such as the α particle and heavier particles are forbidden. On the other hand, since the Q values for α fragments in most light nuclei are larger than those for other cluster decay channels, α decay is favored in the statistical decay process.

In the present work, particle decays from the quasifree proton-knockout reactions on ^{12}C and ^{16}O are studied to understand the structures and fragmentation mechanisms of the s-hole states in ^{11}B and ^{15}N. The $(p, 2p)$ reaction at intermediate energies is well described by the direct reaction picture and is flexible enough to choose the proper kinematics to enhance the s-hole state.

2. EXPERIMENTAL PROCEDURE AND RESULTS

The experiment was carried out at the Research Center for Nuclear Physics (RCNP), Osaka University, by using a 392-MeV proton beam accelerated by the AVF and Ring cyclotrons. The quasifree $(p, 2p)$ reaction was measured with the dual spectrometer system consisting of the high-resolution spectrometer Grand Raiden (GR) [10] and the large-acceptance spectrometer (LAS) [11]. GR was set at the most possible forward angle (25.5°) for the $(p, 2p)$ mode and detected protons with higher energies, taking into account the difference of the momentum acceptance of GR (5%) and LAS (30%). The laboratory angle of LAS and the magnetic fields of the spectrometers were determined to satisfy the zero-recoil momentum condition at the central energy of the $1s_{1/2}$-knockout bump, where the cross section leading to the s-hole state is maximal. Two multiwire drift chambers in each focal plane of both spectrometers determined the positions and the incidence angles of particles. Particle identification was provided by the ΔE signals from plastic scintillation counters, which were also used for trigger signals. We separated the experiment into two parts. In the first beam time, charged particle decay of the s-hole states in both ^{11}B and ^{15}N was measured in coincidence with the quasifree ^{12}C$(p, 2p)$ and ^{16}O$(p, 2p)$ reactions, and neutron decay of the s-hole state in ^{15}N was measured in the second beam time.

In the measurements of charged-particle decay, one generally needs a thin target because the energy losses of the emitted particles like α in the target are not negligible. We used a natural carbon target with a thickness of 0.5 mg/cm^2 for the ^{12}C$(p, 2p)$ reaction. A quartz glass (SiO_2) target and a natural silicon (Si) target each with thickness of about 2 mg/cm^2 were employed for the ^{16}O$(p, 2p)^{15}$N reaction, and the cross section was obtained after subtracting the Si target runs from the SiO_2 runs. Charged particles decaying from the highly excited states in ^{11}B and ^{15}N were measured in sixteen telescopes of ΔE–E Si solid-state detectors (SSD) in coincidence with the two protons of the $(p, 2p)$ reaction. Each telescope consisted of a thin (20, 50, or 100 μm) ΔE SSD and a thick (5000 μm) E Si(Li) detector. Eight 20-μm ΔE detectors were used for the identification of α particles with $E_\alpha \geq 4.5$ MeV. The 50-μm and 100-μm ΔE detectors were used for identification of protons, deuterons, and tritons. The SSD telescopes were mounted on a copper frame of a hemispherical shape and placed in the scattering chamber at backward angles. The total solid angle of the SSD array was 3.5% of 4π. In order to reduce the leakage current, the SSD system was cooled to about −20°C with four Peltier elements. The experimental details and the results for the charged-particle decay of the ^{11}B(s-hole) state were already reported in [12].

In the measurements of neutron decay, we used a newly constructed small scattering chamber made of thin stainless steel with a 4-mm thickness and a neutron multidetector array system previously developed at RCNP [13], which consisted of, at maximum, 48 BC-501A liquid scintillators. In the present experiment, 30 scintillators were employed and placed at a distance of 2 m from the target. The energy of each neutron was determined with the time-of-flight (TOF) methods. The neutron-decay measurements were carried out only for the ^{16}O$(p, 2p)$ reaction. In the detection of decay neutrons, the thickness of the target is not a serious problem, but the detection efficiency and the solid angle are small compared to the charged-particle decay measurements. Therefore, we adopted an H_2O ice sheet as a background-free oxygen target, which was recently developed by Kawabata *et al.* [14]. The ice target with a thickness of 40 mg/cm^2 was cooled down to below 140 K by liquid nitrogen, where the loss of the target material by the sublimating process is negligible.

Excitation energy spectra of the hole states obtained by summing up the energies of two emitted protons are shown in Fig. 1*a* for the ^{12}C$(p, 2p)^{11}$B reaction and in Fig. 2*a* for the ^{16}O$(p, 2p)^{15}$N reaction. The differential cross sections are calculated with $\Delta\Omega_1 = 4.3$ msr, $\Delta\Omega_2 = 20.0$ msr, and $\Delta E_1 = 12.5$ MeV. The systematic errors of the absolute cross sections are estimated to be 10 to 15%, which are due

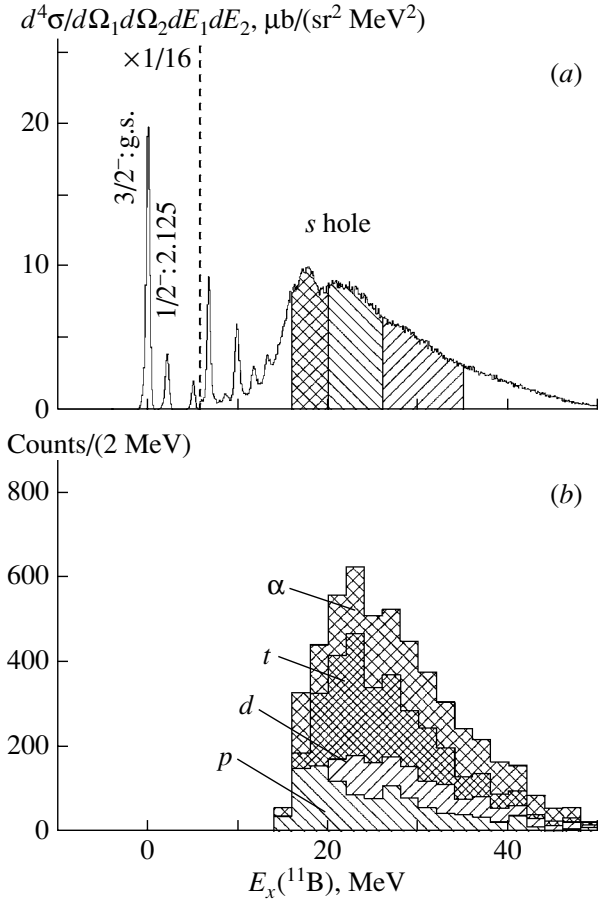

Fig. 1. (*a*) Energy spectrum of the differential cross section of ^{11}B produced by the ^{12}C$(p, 2p)^{11}$B* reaction at $E_p = 392$ MeV. (*b*) Excitation energy spectra of ^{11}B in coincidence with decay charged particles. The contributions of the p, d, t, and α decays are shown separately.

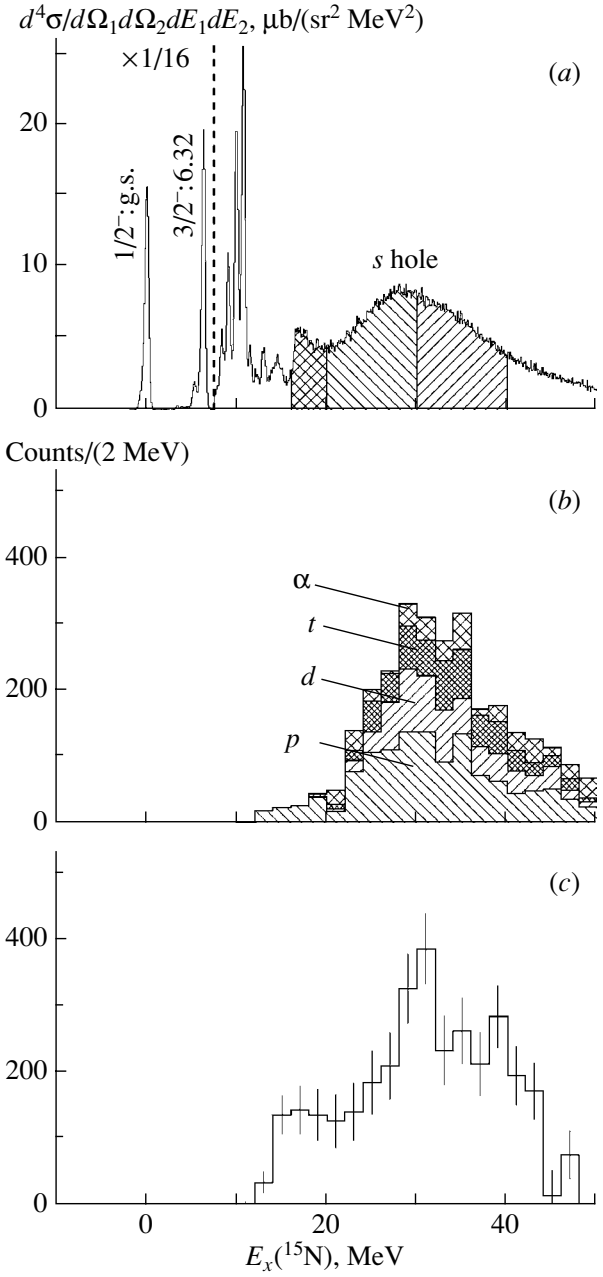

Fig. 2. (*a*) Energy spectrum of the differential cross section of ^{15}N produced by the ^{16}O$(p, 2p)^{15}$N* reaction at $E_p = 392$ MeV. (*b*) Excitation energy spectra of ^{15}N in coincidence with decay charged particles. The contributions of the p, d, t, and α decays are shown separately. (*c*) Excitation energy spectrum of ^{15}N in coincidence with decay neutrons.

to the uncertainties of the target thickness (including contaminant subtractions) and charge collections and the acceptance normalization. Several discrete p-hole states, such as the ground state ($3/2^-$) and the first excited state (2.125 MeV, $1/2^-$) in ^{11}B and the ground state ($1/2^-$) and the third excited state (6.32 MeV, $3/2^-$) in ^{15}N, are observed with an energy resolution of 450 keV (FWHM). The s-hole states are strongly excited in the higher excitation energy region. The bump corresponding to the s-hole state in both ^{11}B and ^{15}N obviously splits into several components.

In the higher end of excitation energies, the detection efficiencies decrease gradually in both reactions due to the finite momentum acceptance of the spectrometers. Moreover, in the decay measurements, the decay particles were detected mostly for excitation energy above ~ 16 MeV. Therefore, the hatched regions of the s-hole states in both Fig. 1*a* and Fig. 2*a* are studied in the decay analysis, which are further separated into three regions in order to investigate the substructures of the s-hole states.

The coincidence spectra with decay charged particles for the ^{12}C$(p, 2p)$ reaction are shown in Fig. 1*b*. Accidental coincidence events were subtracted. The

threshold energies of two-body decay from ^{11}B to the channels $^{10}\mathrm{B}+n$, $^{10}\mathrm{Be}+p$, $^{9}\mathrm{Be}+d$, $^{8}\mathrm{Be}+t$, $^{8}\mathrm{Li}+{}^{3}\mathrm{He}$, and $^{7}\mathrm{Li}+\alpha$ are 11.5, 11.2, 15.8, 11.2, 27.2, and 8.7 MeV, respectively. The ^{3}He-decay events, which are hardly expected due to its large threshold energy, are included in the α-decay portion. It is apparent in Fig. 1*b* that the triton contribution is the largest, although the Q value is smaller than that of α decay. The branching ratios are calculated under the assumption that the decay from the s-hole state is isotropic:

$$\mathrm{Br}_i = \frac{\int n_i(4\pi/\Delta\Omega_{\mathrm{SSD}})dE_x}{\int N dE_x}, \qquad (1)$$
$$i = (n), p, d, t, \text{ and } \alpha,$$

where N is the number of events of the $(p,2p)$ reaction, n_i is the number of particles detected for i decay, and E_x is the excitation energy of the s-hole state.

From the projection of two-dimensional spectra of the energies of decay particles versus the excitation energy E_x of ^{11}B, the peaks populating low-lying states up to the excitation energy of about 5 MeV in each residual daughter nucleus indicate that those events occur mainly through a binary decay process. We define the two-body decay region in each decay channel of the ^{11}B(s-hole) state as $E_x(\mathrm{res}) \leq \max(5\ \mathrm{MeV}, E_{\mathrm{th}}(3\text{-body}))$, where E_x(res) indicates the excitation energy relative to the ground state and E_{th}(3-body) denotes the threshold energy of particle decay in the residual nucleus. The branching ratio of the two-body decay to the low-lying states of the residual nucleus is calculated for this region. Events outside of the two-body decay region consist of mainly the three-body decay and sequential decay processes. It should be noted that, for particles with small E_{th}(3-body), the three-body decay and sequential decay processes are partially included in the two-body decay region defined above.

The coincidence spectra with decay particles for the $^{16}\mathrm{O}(p,2p)$ reaction are shown in Figs. 2*b* and 2*c* for charged particles and neutrons, respectively. The threshold energies of two-body decay from ^{15}N to the channels $^{14}\mathrm{N}+n$, $^{14}\mathrm{C}+p$, $^{13}\mathrm{C}+d$, $^{12}\mathrm{C}+t$, $^{12}\mathrm{B}+{}^{3}\mathrm{He}$, and $^{11}\mathrm{B}+\alpha$ are 10.8, 10.2, 16.2, 14.8, 28.2, and 11.0 MeV, respectively. The ^{3}He-decay events are also included in the α-decay portion. In Fig. 2*b*, it is found that the α-decay contribution is very small. The branching ratios are calculated using Eq. (1) for the range between 16 and 40 MeV. In the region of $E_x \leq 20$ MeV, however, d and t decays could not be measured due to the lower limits of the detectable energies. The branching ratios of the decay to the low-lying states of the residual nuclei are calculated similarly in the case of ^{11}B. The two-body decay region in each decay channel is defined as $E_x(\mathrm{res}) \leq \max(8\ \mathrm{MeV}, E_{\mathrm{th}}(3\text{-body}))$. The three-body decay and sequential decay processes are almost excluded in the two-body decay region, except for d decay with the three-body decay threshold energy of 5.0 MeV.

3. COMPARISON WITH THEORETICAL CALCULATIONS

In Fig. 3, the experimental branching ratios of decay particles from the excitation energy region of 16–35 MeV in ^{11}B and of 20–40 MeV in ^{15}N are shown, respectively, together with the results of a statistical-model calculation with the code CASCADE [15]. The transmission coefficients were calculated with the global optical potential parameters of [16–20], which are well suited for light nuclei. Energy levels known below 12-MeV excitation energy were explicitly included for all nuclei ($6 \leq A \leq 16$) necessary for the calculation, while the levels of higher excitation energies were calculated using level-density parameters given in the code. In the CASCADE calculations, decay particles above the experimental detection thresholds were only employed to obtain the branching ratios. The branching ratios of the decay onto the two-body decay regions are also indicated in Fig. 3 with dark areas.

In the case of the ^{11}B(s-hole) state, the measured branching ratios of both t decay and α decay are much larger than those of the statistical-model calculations. The experimental α decay in the two-body decay region is about one-half of the total α decay, indicating that contributions of the sequential decay and three-body decay processes are large in this channel. Actually, the $\alpha+\alpha+t$ three-body decay channel has a very low threshold energy of 11.2 MeV and may compete against the two-body decay process, while the statistical-model calculations include only the two-body decay and sequential decay processes. This suggests that the three-body decay process could contribute significantly to the branching ratios of α decay. However, even in the two-body decay regions, the t-decay strength is still dominant. Furthermore, the relative ratio of the t decay to the α decay in the experiment is opposite to that of the statistical calculations as well as the ratio of the p decay to the d decay.

In the case of the s-hole state in ^{15}N, the three-body decay threshold is higher than those of the two-body n, p, d, t, and α decay. Moreover, the ground state of ^{16}O is more purely described as the $SU(3)(\lambda\mu) = (00)$ state. Thus, ^{15}N is more suitable to understand the microscopic structure and fragmentation mechanism of the s-hole state. In Fig. 3

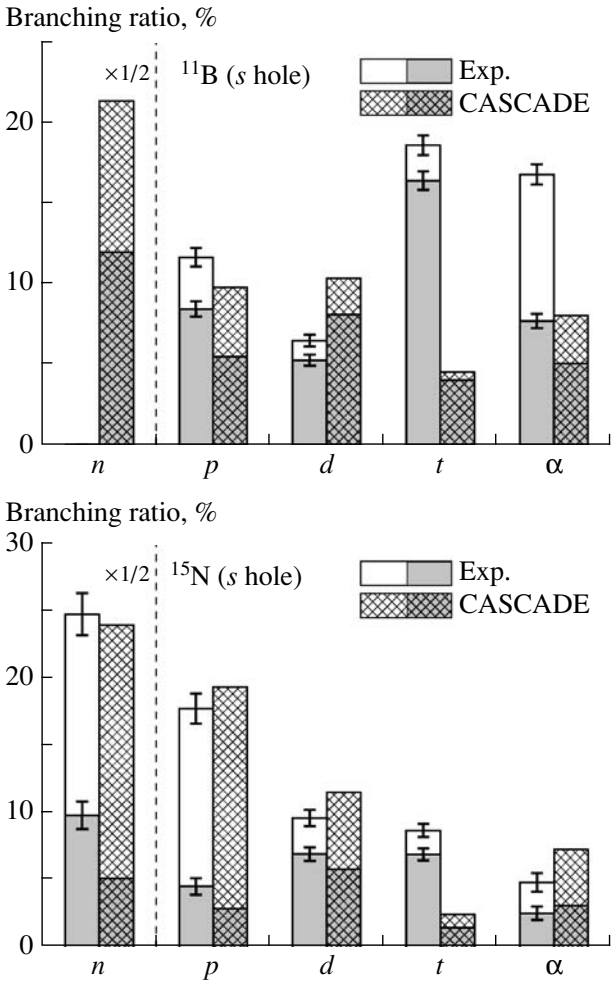

Fig. 3. Comparisons of the measured branching ratios of the n, p, d, t, and α decays from the excitation energy region of 16–35 MeV in ^{11}B and of 20–40 MeV in ^{15}N with those of the statistical-model calculation using the code CASCADE. The error bars shown include only statistical errors. The experimental branching ratio of the n decay is measured only for the ^{15}N(s-hole) state. The branching ratios of the decay onto the two-body decay regions are indicated with dark areas (see text).

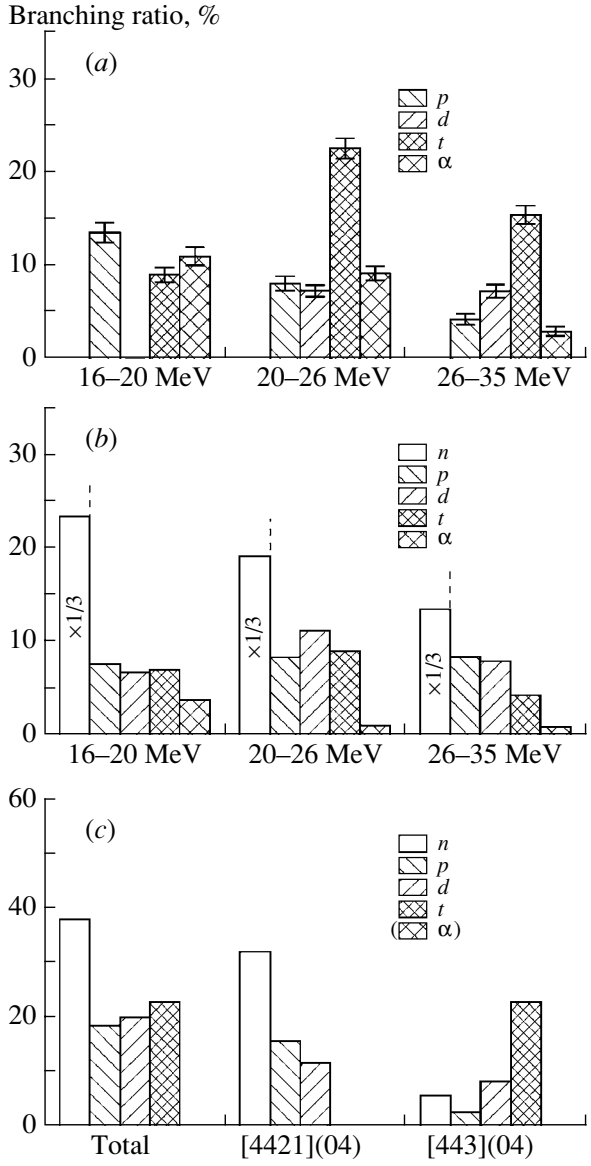

Fig. 4. (a) Experimental branching ratios of the p, d, t, and α decays onto the two-body decay regions from the three excitation energy regions of 16–20, 20–26, and 26–35 MeV in ^{11}B. (b) Branching ratios of the n, p, d, t, and α decays from the three excitation energy regions of 16–20, 20–26, and 26–35 MeV in ^{11}B obtained by the $1\hbar\omega$ shell-model calculations [21]. (c) Branching ratios of the n, p, d, t, and α decays from the doorway s-hole state in ^{11}B calculated by the $SU(3)$ model [9]. Branching ratios for the states with $[f](\lambda\mu) = [4421](04)$ and $[f](\lambda\mu) = [443](04)$ and total branching ratios are shown.

(bottom), the neutron fragments account for about half of the total decay fragments in both the measurements and the statistical-model calculations. Only the measured branching ratio of t decay is much larger than that of the statistical-model calculations. The n decay and p decay are considerably reduced in the two-body decay regions, suggesting the sequential decay processes are large in these channels. In the two-body decay regions, the measured n decay and t decay are larger than those of the statistical-model calculations, while the measured p, d, and α decays are reasonably well explained by the calculations. Although the large t decay compared to α decay supports the selection rule coming from the $SU(3)$ spatial symmetry, the portion of the statistical decay may be considerable for the ^{15}N(s-hole) state.

Figure 4a shows the branching ratios of p, d, t, and α decays in the two-body decay regions from the three excitation energy regions of 16–20, 20–

26, and 26–35 MeV in ^{11}B. The decay patterns from the respective regions suggested by the substructures are very different, indicating that the s-hole state in ^{11}B splits into some components with different microscopic structures. Owing to the detection threshold, the measured deuteron branching ratio is zero in the low-energy region. Predictions from the $SU(3)$ model [9] are shown in Fig. 4c, where the ^{11}B(s-hole) state has the same spatial symmetry as the ground state of ^{12}C, $SU(3)(\lambda\mu) = (04)$, and has two degenerated partition symmetries $[f] = [443]$ and $[4421]$. When the branching ratios of α decay are neglected, the experimental decay pattern of the 26–35 MeV region is similar to that of the $SU(3)[f](\lambda\mu) = [443](04)$ component. The first and second regions may have both the $SU(3)[f](\lambda\mu) = [4421](04)$ and $[443](04)$ components, whereas the mixing of the $[4421](04)$ component seems to decrease with increasing excitation energy.

Yamada [21] has recently made new calculations within the framework of the $1\hbar\omega$ shell model. The excitation spectrum of the ^{12}C$(p, 2p)$ and ^{16}O$(p, 2p)$ reaction was formulated within the impulse approximation, where calculated energy-dependent spectroscopic factors for the ^{12}C(g.s.) $\rightarrow p + {}^{11}$B(s-hole) and ^{16}O(g.s.) $\rightarrow p + {}^{15}$N(s-hole) processes were folded by a Lorentzian function. The result of the shell-model calculation shows that the s-hole state in ^{11}B splits into three parts. Although the calculated strength ratios of the three regions are different from the experimental results, the substructure of the s-hole state is reasonably well explained by the shell-model calculation. The energy dependence of the branching ratios for n, p, d, t, and α decays from the ^{11}B(s-hole) state was also calculated using the separation-energy method [22], where the partial decay width is defined as the product of the penetration factor and reduced width. As shown in Fig. 4b, the calculated branching ratio of the t decay is larger than that of the α decay, reflecting the selection rule as mentioned above. The enhancement of the t decay observed in the present experiment, however, is not reproduced by the shell-model calculation. Calculations including the direct three-body decay process will be needed to explain the experimental decay pattern.

Figure 5a shows the experimental branching ratios of n, p, d, t, and α decays in the two-body decay regions from the three excitation energy regions of 16–20, 20–30, and 30–40 MeV in ^{15}N. The decay patterns between the lower region and higher region of the bump with the mean energy of 28 MeV are very different, indicating that this s-hole bump in ^{15}N includes a few components with different microscopic

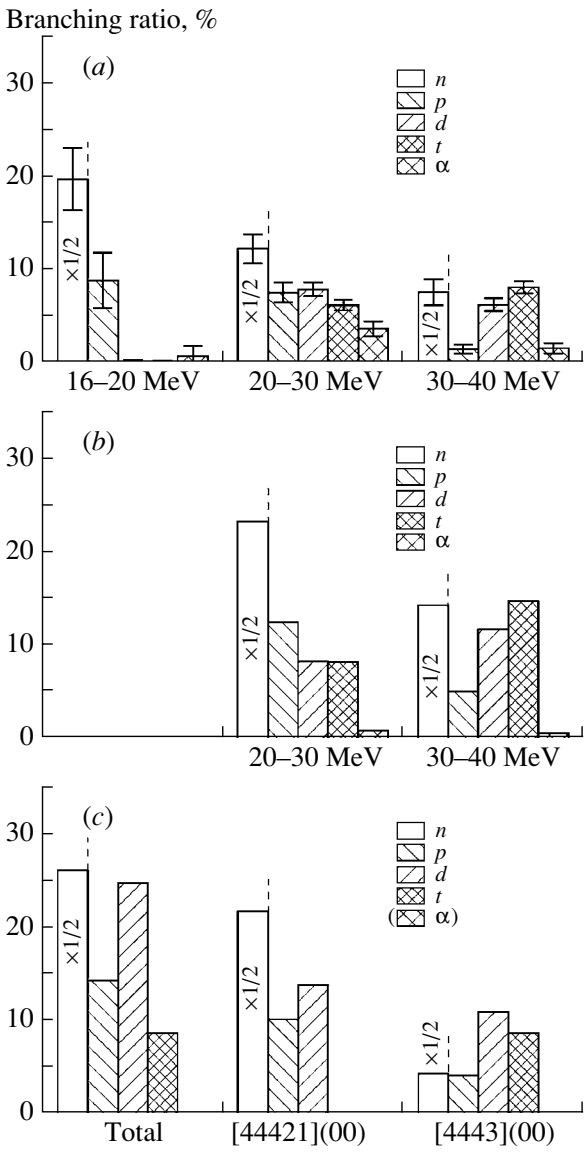

Fig. 5. (a) Experimental branching ratios of the n, p, d, t, and α decays onto the two-body decay regions from the three excitation energy regions of 16–20, 20–30, and 30–40 MeV in ^{15}N. (b) Branching ratios of the n, p, d, t, and α decays from the two excitation energy regions of 20–30, and 30–40 MeV in ^{15}N obtained by the $1\hbar\omega$ shell-model calculations [21]. (c) Branching ratios of n, p, d, t, and α decays from the doorway s-hole state in ^{15}N calculated by the $SU(3)$ model [9]. Branching ratios for the states with $[f](\lambda\mu) = [44421](00)$ and $[f](\lambda\mu) = [4443](00)$ and total branching ratios are shown.

structures. Predictions from the $SU(3)$ model [9] are shown in Fig. 5c, where the ^{15}N(s-hole) state has the same spatial symmetry as the ground state of ^{16}O, $SU(3)(\lambda\mu) = (00)$, and has two degenerated partition symmetries $[f] = [4443]$ and $[44421]$. The branching ratio of α decay is exactly zero in the calcu-

lations of the $SU(3)$ model due to the selection rule. The experimental decay pattern of the 30–40 MeV region strongly supports the selection rule and is similar to that of the $SU(3)[f](\lambda\mu) = [4443](00)$ component. However, the large branching ratios of d decay in the $SU(3)$-cluster model calculations do not agree with the experimental branching ratio, even taking into account the rather large lower limit of the detection energy. The second region may have both the $SU(3)[f](\lambda\mu) = [44421](00)$ and $[4443](00)$ components.

The branching ratios for two energy regions calculated with the shell model are shown in Fig. 5*b* for n, p, d, t, and α decays from ^{15}N(s-hole) state. The branching ratio of the α decay is very small owing to the selection rule as mentioned above. The agreement between the experimental branching ratios onto the two-body decay regions and calculated ones is fairly good in both regions, implying that the main part of the binary fragmentation is the direct decay of the doorway s-hole state. At first sight, this seems to be inconsistent with the results obtained from the comparison with the statistical-decay calculations, where some (not small) amounts of the statistical decay are considered to contribute to the total branching ratios. However, if we estimate the direct decay parts of the experimental branching ratios by subtracting the calculated statistical-decay ratios multiplied by 0.5 from the experimental ones in the two-body decay regions and compare it with the result of the shell-model calculations of Fig. 5*b* multiplied by 0.5, the agreement between two branching ratios is very good not only for the decay patterns but also for the absolute values. This indicates that the ratio of the escape width ($\Gamma^{\uparrow}$) to the spreading width ($\Gamma^{\downarrow}$) of the ^{15}N(s-hole) state is about 1.

4. SUMMARY

We presented the first measurements of the decay particles from the s-hole state in ^{11}B and ^{15}N excited by the ^{12}C$(p, 2p)$ and ^{16}O$(p, 2p)$ reactions at $E_p =$ 392 MeV. The measured excitation energy spectra show that both s-hole states split into some substructures. These splittings agree qualitatively with the results of recent shell-model calculations [21]. For the s-hole state in ^{11}B, the triton decay probability was found to be larger compared to any other decay, although the Q value of the α-decay channel is larger. The present results for the decay branching ratios of the ^{11}B(s-hole) state cannot be reproduced by statistical model calculations. $SU(3)$-model calculations [9] explain the experimental decay character qualitatively in the higher excitation region, while the $SU(3)(\lambda\mu) = [443](04)$ feature in the $SU(3)$-model calculations becomes unclear in the shell-model calculations.

In the case of the s-hole state in ^{15}N, the suppression of α decay is clearly recognized in the binary decay process, which supports the selection rule due to the spatial $SU(3)$ symmetry. The shell-model calculation explains the experimental two-body decay patterns better than the $SU(3)$-model calculations. From a comparison between the experimental results and both the statistical-model and the shell-model calculations, nearly half of the total fragmentation of the ^{15}N(s-hole) state is concluded to be the direct decay of the doorway s-hole state.

ACKNOWLEDGMENTS

We are grateful to the RCNP cyclotron staff for preparing a stable and clean beam. We thank K. Ikeda for fruitful discussions and encouragement.

This research was supported in part by the Grant-in-Aid for Scientific Research no. 09440105 and for the 21st Century COE "Center for Diversity and Universality in Physics" from the Japanese Ministry of Education, Sports, Culture, Science, and Technology.

REFERENCES

1. O. Chamberlain and E. Segrè, Phys. Rev. **87**, 81 (1952).
2. G. Jacob and T. A. J. Maris, Rev. Mod. Phys. **45**, 6 (1973), and references therein.
3. S. L. Belostotskii *et al.*, Yad. Fiz. **41**, 1425 (1985) [Sov. J. Nucl. Phys. **41**, 903 (1985)]; S. S. Volkov *et al.*, Yad. Fiz. **52**, 1339 (1990) [Sov. J. Nucl. Phys. **52**, 848 (1990)].
4. S. Frullani and J. Mougey, Adv. Nucl. Phys. **14**, 1 (1984), and references therein.
5. H. Bando, T. Yamada, and J. Žofka, Phys. Rev. C **36**, 1640 (1987).
6. T. Yamada and K. Ikeda, Prog. Theor. Phys. Suppl. **117**, 445 (1994).
7. H. Ejiri, Phys. Rev. C **48**, 1442 (1993).
8. Y. Hayato *et al.* (The Super-Kamiokande Collab.), Phys. Rev. Lett. **83**, 1529 (1999).
9. T. Yamada, M. Takahashi, and K. Ikeda, Phys. Rev. C **53**, 752 (1996).
10. M. Fujiwara *et al.*, Nucl. Instrum. Methods Phys. Res. A **422**, 484 (1999).
11. N. Matsuoka *et al.*, RCNP Annual Report (1991), p. 186.
12. M. Yosoi *et al.*, Phys. Lett. B **551**, 255 (2003).
13. T. Inomata *et al.*, Phys. Rev. C **57**, 3153 (1998).
14. T. Kawabata *et al.*, Nucl. Instrum. Methods Phys. Res. A **459**, 171 (2001).
15. F. Pühlhofer, Nucl. Phys. A **280**, 267 (1977); M. N. Harakeh, *Extended Version of Code CASCADE* (1983) (unpublished).

16. D. Wilmore and P. E. Hodgson, Nucl. Phys. **55**, 673 (1964).
17. B. A. Watson, P. P. Singh, and R. E. Segel, Phys. Rev. **182**, 977 (1969).
18. F. Michel *et al.*, Phys. Rev. C **28**, 1904 (1983).
19. M. Ermer *et al.*, Nucl. Phys. A **533**, 71 (1991).
20. J. B. A. England *et al.*, Nucl. Phys. A **475**, 422 (1987).
21. T. Yamada, Nucl. Phys. A **687**, 297c (2001).
22. H. Horiuchi, K. Ikeda, and Y. Suzuki, Prog. Theor. Phys. Suppl. **52**, 89 (1972).